Iranian Polymer Journal (2018) 27:795–806
https://doi.org/10.1007/s13726-018-0652-3

ORIGINAL RESEARCH

Boron-containing UV-curable oligomer-based linseed oil as flame-retardant coatings: synthesis and characterization

Deepak M. Patil[1] · Ganesh A. Phalak[1] · Shashank T. Mhakse[1]

Received: 7 November 2017 / Accepted: 29 July 2018 / Published online: 27 August 2018

Abstract

A boron-containing UV-curable oligomer was derived from linseed oil, phenylboronic acid and glycidyl methacrylate to use in flame-retardant coating applications. The synthesized UV-curable oligomer was characterized for its structural and physicochemical properties by means of Fourier transform infrared (FTIR), ^{1}H and ^{11}B-nuclear magnetic resonance (NMR) spectroscopy techniques. The boron-containing UV-curable oligomer (BELO) was added to a conventional polyurethane acrylate (PUA) at varying concentrations ranging from 10 to 40 wt% in the presence of a photoinitiator and a reactive diluent. LOI and UL-94 tests were performed to understand the flame-retardancy behavior of the synthesized BELO oligomer, and the results revealed that the flame retardancy of UV-curable coatings enhanced as the percentage of BELO oligomer in the coating formulations increased. The glass transition temperature (T_g) and thermal stability of cured coatings were analyzed by differential scanning calorimetry and thermogravimetric analysis, respectively. The TGA analysis showed that char yield at 600 °C increased by increasing the BELO oligomer content. The mechanical properties, and stain, solvent, and chemical resistance and thermal behavior of the coatings were investigated. Incorporation of BELO into the PUA coating formulations and the comparison of the properties of BELO-incorporated PUA coatings with those of the conventional PUA coating exhibited interesting results.

Keywords Linseed oil · Epoxidation · Boron · UV-curing · Flame retardant

Introduction

Wood structural backbone is made of carbonaceous cellulose materials, and therefore, it is prone to fire accidents. Thus, it is necessary to improve the fireproof capability of wood-based material and to develop suitable flame-retardant materials which would enhance the fire-resistance properties of wood materials [1]. Fire-resistance properties can be improved by adding flame-retardant (FR) materials which have physical or chemical interactions with wood-based material. They can be incorporated into the backbone to delay the burning process of materials by enhancing the foam ignition temperature or reducing the rate of flame spread. The physically added flame-retardant additives show effective flame retardancy at higher concentrations and lead to adverse effects on coating properties, such as mechanical, chemical, solvent and thermal stability. The chemically reactive flame-retardant additives show effective flame retardancy at lower concentrations, and hence, causing less damage to the coating properties and reducing the migration of additive to the material surface, which generally occurs for physically added flame-retardant additives [2]. Nowadays, halogen- and phosphorus-containing reactive flame retardants are used to improve the fire-resistance properties [3–5]. These reactive flame retardants have various drawbacks, which are responsible for corrosive smoke and ejection of extremely carcinogenic substances like dibenzodioxins and dibenzofurans. Smoke adversely affects human health and poses pollution problems when it is released into the environment [6]. Therefore, considering the environmental and human health-related issues, the scientific community has focused on the environmentally friendly flame-retardant materials [7, 8]. Boron-containing flame retardants, such as boric acid and its analogous have been in use for a long time [9]. Organoboron flame retardants lose their water molecules, and finally, convert to boron oxide. Boron oxide

✉ Shashank T. Mhakse
stmhaske@ictmumbai.edu.in

[1] Department of Polymer and Surface Engineering, Institute of Chemical Technology, Nathalal Parekh Marg, Matunga (E), Mumbai 400019, India

which is formed during the degradation process is the result of cleavage in B–C and B–O–C bonds. The pyrolysis mechanism of boron oxide is well-known in the literature and it has been considered that they do not generate the corrosive or hazardous smoke during combustion as halogenated flame retardant [1]. Thus, boron-based compounds are considered as an environmentally friendly flame retardant and a good alternative for halogenated-based flame retardants. Boron-based compounds can act as an effective flame retardant due to their ability to form an impermeable glassy coating layer upon their degradation. The glassy coating formed on the surface of polymeric materials acts as a protective barrier and facilitates the exclusion of oxygen and prevents further propagation of combustion. Upon thermal decomposition, boron-containing flame retardants produce boron oxide in the condensed phase and alter the decomposition process of the polymer in favor of carbonaceous char rather than CO or CO_2 [10, 11].

Environmental concerns and health-related issues have stimulated researchers to develop environment-friendly coatings with low or zero VOC content [12]. In this sense, researchers have developed high solids, water dispersible [13], powder [14], and radiation (UV/EB) curing coatings [15, 16], which have low VOC contents. UV-curing technology has zero VOC content and it has been used in protective coatings, printing inks, adhesives, varnishes, and composites due to its shorter reaction time, lower energy consumption, and economically favorable and environmentally friendly aspects [17, 18]. Nowadays, UV-curable epoxy acrylate, PUA, and acrylic resins are readily available in the market, however, amongst them, PUA has attracted great interest in the coatings and adhesives due to its outstanding adhesion, excellent flexibility, and chemical resistance ability. PUA resins are usually prepared by the reaction of polyol and hydroxyl functional acrylic monomers with diisocyanate, yielding double bond-terminated resin as product [19]. Furthermore, most of the PVA resins are obtained from petroleum-based materials which have limited availability [20]. The petroleum based raw materials have limited sources and if we didn't find the alternative sources it may be finished. Therefore, increasing the worldwide interest to utilize the renewable resources which are abundantly available in nature to synthesize the resins [21, 22]. In this regard, many research works have been done on the utilization of renewable resources for synthesizing resins, such as epoxy [23, 24], polyester [25, 26], polyurethane [27], and polyesteramide [28]. These resins have become an environmentally possible substitute to petrochemical-based materials in coating industry [29]. In this context, many kinds of renewable raw materials, such as plant oils, rosins, terpenes, and sugars have been used for building blocks of polymeric materials [30, 31]. Vegetable oils (both edible and non-edible) are one of the cheapest and most abundant biological feedstocks available in large quantities, and their use as starting materials offers numerous advantages, such as low toxicity and inherent biodegradability [32]. Marta et al. synthesized a boron-containing flame retardant thermosetting copolymer by cationic polymerization from soybean oil. LOI measurements were carried out and it was observed that LOI values increased from 19.2 for the boron-free system to 25.6 as the boron content was increased in the system [33]. Emrach et al. pioneered boron-containing flame retardant coatings by thiol-ene polymerization reaction. 4-Vinylphenyl boronic acid was used to provide the flame-retardancy properties to the coatings [34]. In a further study, biodegradable flame-retardant UV-curable sol/gel-based coatings were prepared from methacrylated and phosphorylated epoxidized soybean oil. Liquid UV-curable coating materials were applied on polycarbonate substrate and it was cured with UV light. Their flame-retardancy performances were determined, and the results showed that the incorporation of sol–gel precursor into the resin led to an enhancement in the thermal stability and flame retardancy of the coated materials [35]. In our previous work, we successfully synthesized an UV-curable PUA resin from a polyol derived from itaconic acid (IA) as a renewable resource, isophorone diisocyanate (IPDI) and 2-hydroxylethyl methacrylate (HEMA). The combination of renewable resources and UV-cured coatings provides a greener protocol which has a bright future in industry [36]. In this work, the combination of a renewable resource and an UV-cured coating system was used to synthesize flame-retardant coatings with boron as the backbone for flame-retardant application. The novelty of the work is to provide eco-friendly, non-hazardous flame-retardant coatings synthesized from phenylboronic acid and a renewable resource, i.e., linseed oil. The effect of concentration of a boron-based UV-curable oligomer (BELO) has been studied to obtain the best possible formulation for the flame-retardant applications. The molecular structure of boron-containing flame-retardant oligomer was characterized by physicochemical and FTIR, ^{1}H NMR, and ^{11}B NMR spectroscopy analyses. The synthesized boron-containing oligomer was added in various proportions (between 10 and 40 wt%) in the PUA resin formulation, and different flame-retardant UV-curable wood coatings were prepared. The effects exhibited by BELO oligomer on the flame-retardant performance have been presented and discussed in terms of LOI and UL-94 tests results.

Experimental

Materials

Linseed oil (LO), sodium hydroxide, sodium chloride, hydrogen peroxide (H_2O_2, 30%), triethylamine, sulphamic

acid (H_3NSO_3), and acetic acid were purchased from S.D. Fine Chem. Ltd., Mumbai. Phenylboronic acid and glycidyl methacrylate (GMA) were purchased from Sigma-Aldrich Chemicals Pvt. Ltd., Mumbai, India. EBECRYL 8405, an aliphatic urethane acrylate (PUA) (functionality: 4, density: 1.13 g/mL, and viscosity at 60 °C: 4500 cP/mPa s), was received from Allnex Resins Pvt Ltd., India. The acid form of sulfonated polystyrene-type ion exchange resin, Amberlite IR-120H, from Rohm Hass Co. (Philadelphia, PA, USA) was used as the catalyst. The photoinitiator 2-hydroxy-1-{4-[4(2-hydroxy-2-methyl-propionyl)-benzyl]-phenyl}-2-methyl-propan-1-one (IRGACURE 127) was received from BASF, India. Dipropylene glycol diacrylate (Photomer 4226) as reactive diluent was received from Shepherd Color Company, India. All materials were used as received without any further purification.

Synthesis of epoxidized linseed oil (ELO)

During epoxidation reaction, the molar ratio of carbon double bonds to acetic acid to hydrogen peroxide was 1:0.5:1.5 and this was maintained throughout the reaction. A four-necked flask equipped with a mechanical stirrer, thermometer packet, and a reflux condenser was charged with LO, Amberlite IR-120H and acetic acid. The reaction mixture temperature was raised gradually from ambient to 55 °C to start the epoxidation reaction, and then, hydrogen peroxide (30%) was added gradually to the reaction mixture for about 1 h. The reaction mixture was allowed to heat for next 6 h for completion of the reaction. The synthesized ELO was separated from the reaction mixture and then characterized by FTIR and ^{1}H NMR analyses.

Synthesis of phenylboronic methacrylate (PBMA) oligomer

A 250 mL three-necked round bottom flask equipped with magnetic stirrer was charged with 26.91 g (0.1893 mol) of GMA and sulphamic acid as a catalyst (0.5 mol%) in THF (50 mL). The reaction mixture was stirred gradually and the solution of 23.08 g (0.1893 mol) PBA and triethylamine (1 mol%) in THF was added dropwise over a period of 1 h. After completion of the addition, the reaction was continued for the next 24 h at room temperature to achieve complete conversion. After completion of the reaction, the catalyst was filtered out and solvent was removed under reduced pressure with the help of a rotary evaporator. Finally, a yellowish liquid product was collected, and then, characterized by FTIR and ^{1}H NMR analyses.

Synthesis of boron-containing epoxidized linseed oil (BELO) oligomer

A mixture of ELO and PBMA was added in a four-necked flask which was equipped with a water condenser, and magnetic stirrer. The reaction conditions for BELO oligomer synthesis were very similar to those discussed for PBMA oligomer synthesis. The synthesized BELO oligomer was separated out from the reaction mixture, and characterized by iodine value, FTIR, ^{11}B and ^{1}H NMR analyses.

Preparation of UV-curable flame-retardant coatings for wood substrate

Boron-containing UV-curable flame-retardant coatings for wood substrate formulations were prepared by the addition of BELO oligomer at the various concentrations listed in Table 1. Each formulation was prepared in a beaker with vigorous stirring and the prepared formulations were coated onto wood panels (10 cm × 7 cm) using a bar applicator. Free films were prepared by pouring the formulation mixture onto Teflon molds. The panels were cured by an UV-curing machine (UNIQUE UV Curing Machine, India) using a 4 kW high-pressure mercury lamp (30–400 nm wavelength) within almost 20 s exposure time. The UV-cured coatings were evaluated by their solvent and chemical resistance, mechanical, thermal and flame-retardant properties.

Characterization

Iodine value

Wij's method was performed to determine iodine value using iodine monochloride solution in acetic acid and carbon tetrachloride. Then, KI solution was added to determine the excess halogen and the liberated iodine was titrated with sodium thiosulphate solution (ASTM D1959-97):

$$\mathrm{IV} = \frac{(B - S) \times 12.69 \times N}{W}, \quad (1)$$

Table 1 Formulation of UV-curable flame-retardant coatings

Code	PUA oligomer	BELO oligomer	Reactive diluent	Photoinitiator
PUA	76	0	20	4
PUA10	66	10	20	4
PUA20	56	20	20	4
PUA30	46	30	20	4
PUA40	36	40	20	4

where B = burette reading for blank (mL), S = burette reading for sample (mL), N = normality of $Na_2S_2O_3$ solution, W = weight of sample (g).

Epoxy equivalent weight (EEW)

A known weight of the sample was taken in an Erlenmeyer flask, completely dissolved in 25 mL hydrochlorination agent, followed by the addition of bromocresol red as an indicator, and then titrated against 0.1 N NaOH solution:

$$\text{EEW} = \frac{C \times 1000}{(B - S) \times N}, \quad (2)$$

where B = blank burette reading (mL), S = sample burette reading (mL), N = normality of NaOH solution, C = weight of sample (g).

Fourier transform infrared spectroscopy

The chemical structure of ELO, PBMA and BELO oligomer was identified by FTIR analysis on a Bruker ATR spectrophotometer, USA. FTIR absorption spectra were recorded in 4000–600 cm^{-1} wavelength range.

Nuclear magnetic resonance spectroscopy

The chemical structure of ELO, PBMA and BELO oligomer was also confirmed by ^{1}H and ^{11}B NMR spectroscopy analysis performed on a Bruker DPX 800 MHz spectrophotometer (USA) using DMSO as a solvent.

DSC analysis

Differential scanning calorimetry (DSC) analysis was carried out to determine the glass transition temperature (T_g) of cured coating samples on a TA Q100 analyzer, USA. For DSC analysis, each sample was weighed accurately in an aluminum pan and heated in 40–100 °C temperature range using 10°C/min rate of heating.

TGA analysis

Thermal stability of cured coatings was monitored by TGA analysis on a PerkinElmer TGA 4000 instrument (USA) in 40–600 °C temperature range with 20°C/min heating rate. Statistic heat resistance temperature (T_s) was calculated by the following equation:

$$T_s = 0.49\,[T_d5 + 0.6\,(T_d30 - T_d5)]. \quad (3)$$

Coating analysis

The gloss of coating was measured by a Rhopoint gloss meter at 60° angle (ASTM D523-99). Coating hardness was measured by a pencil hardness tester as per ASTM D3363. The cross-cut adhesion test was examined for checking the adhesion properties as per ASTM D3359. The solvent scrub resistance of coatings was examined by rubbing a cloth saturated with MEK solvent as per ASTM D5420-93. The coatings resistance against various stains was determined by ASTM D3023-98. The stains were applied on the coating surface for 24 h, and washed with water, and subsequently with ethanol.

Limiting oxygen index

The flammability of cured samples was studied by LOI test. LOI is defined as the minimum fraction of oxygen in a flowing mixture of oxygen and nitrogen that will just support the flaming combustion.

UL-94 vertical burning test

UL-94 test was carried out to examine the flammability of coating samples as per ASTM D1356. Test samples with dimension of 8 cm × 1 cm × 1 cm were held vertically and ignited using an LPG Bunsen burner.

SEM analysis

The micromorphology image of residual char after UL-94 tests was obtained using a JSM-6380 (JEOL) scanning electron microscope.

Results and discussion

Boron-containing oligomers usually show a three-step synthetic mechanism. The epoxidation of linseed oil was carried out in the presence of hydrogen peroxide, acetic acid, and Amberlite IR120 as catalyst. The progress of linseed oil epoxidation was monitored by change in iodine value, and it was found that the iodine value of linseed oil changed from 160.57 to 15.54 g of I_2/100 g, and its double bond was successfully converted to oxirane ring. The EEW of epoxidized linseed oil after the completion of the reaction was 562.56 g/mol. The BELO was synthesized using a 1:1 molar ratio of ELO:PBMA. The physiochemical analysis of ELO and BELO is shown in Table 2.

Table 2 Physicochemical analysis

Chemical analysis	EEW	Iodine value
ELO	562.56	15.54
BELO	–	137.94

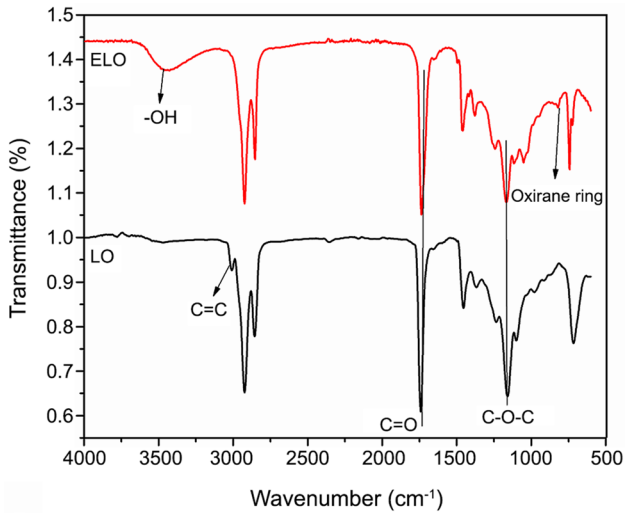

Fig. 1 FTIR analysis of LO, and ELO

FTIR analysis

The FTIR spectra of LO and ELO resins are illustrated in Fig. 1. The absorption peaks at 2923 and 2858 cm^{-1} are attributed to the –CH symmetric and asymmetric stretching vibrations, respectively. The peak observed at 1741 cm^{1} is due to carbonyl (C=O) stretching vibration. The peaks at 1159 and 3008 cm^{-1} are attributed to the C–O–C linkage and unsaturation (–C=C–) of linseed oil, respectively. The peak at 3008 cm^{-1}can be assigned to the unsaturation, which disappeared in the FTIR spectrum of ELO. It is indicated that the unsaturation of linseed oil was converted to oxirane ring in an epoxidation process. In addition, the spectrum shows the additional peaks at 3459 and 826 cm^{-1}, which can be attributed to hydroxyl group and oxirane ring [32, 37]. The FTIR spectra of ELO, PBMA and BELO are also shown in Fig. 2. The FTIR spectrum of PBMA exhibits a peak at 1717 cm^{-1} indicating the presence of carbonyl (C=O) ester. The peaks at 2966 and 2865 cm^{-1} are attributed to the –CH stretching vibration. The spectrum also shows the characteristic peaks at 1310 and 648 cm^{-1}, which are attributed to the –B–O–C– and –B–C– stretching, respectively. The peak at 1160 cm^{-1} is the result of C–O stretching. The characteristic peak at 808 cm^{-1} is attributed to the acrylate unsaturation. The strong band observed at 3335 cm^{-1} reveals the presence of hydroxyl groups and it signifies the reaction of GMA and PBA. The FTIR spectrum of BELO does not show the peak at 826 cm^{-1}, which indicates that all oxirane rings in ELO reacted with the hydroxyl groups of PBMA. The peak at 808 cm^{-1} is attributed to the acrylate C=C bond, which has been successfully incorporated at the end of the BELO oligomer chains [11]. The remaining absorption peaks of BELO are the same as those observed in the ELO and PBMA spectra.

^{1}H NMR analysis

The ^{1}H NMR spectra of ELO, PBMA and BELO are depicted in Fig. 3. The peak at 0.81–0.90 ppm has been attributed to the terminal methyl proton. The absorption peak at 1.26–1.31 ppm corresponds to the protons of all the internal CH_2 groups present in the fatty acid chain. The peak at 1.6–1.638 ppm reveals the proton of the CH_2 group attached next to the terminal methyl group. The proton associated with glyceride moiety has appeared at 4.14–4.32 ppm. The peak at 5.15 ppm corresponds to the proton between the two-glyceride moieties. The characteristic peak at 3.18–2.90 ppm corresponds to the proton of oxirane ring [38]. The ^{1}H NMR spectrum of PBMA oligomer (Fig. 4) shows the peaks at 7.78 and 7.70 ppm which belongs to deshielded aromatic proton. The peaks at 6.05 and 5.95 ppm are attributed to the protons of the vicinal bonds in GMA. The peak observed in the downfield of the spectrum is due to the movement of electrons in the highly delocalized carbon–carbon double bond. The spectrum reveals a singlet at 3.71 ppm which corresponds to the proton of hydroxyl group. Figure 5 shows the ^{1}H NMR spectrum of BELO oligomer, in which the peaks at 7.78 and 7.68 ppm correspond to highly deshielded aromatic proton. The characteristic proton of oxirane ring has a signal at 3.18–2.90 ppm, which has disappeared in the BELO spectrum. A singlet observed at 4.12 ppm corresponds to the proton associated with hydroxyl group. The peaks at 6.72 and 6.54 ppm can be assigned to the protons of the neighboring bonds in PBMA as the end group of BELO [39].

^{11}B NMR analysis

The ^{11}B NMR spectrum in Fig. 6 shows the characteristic peak in the range of 0–20 ppm which corresponds to the

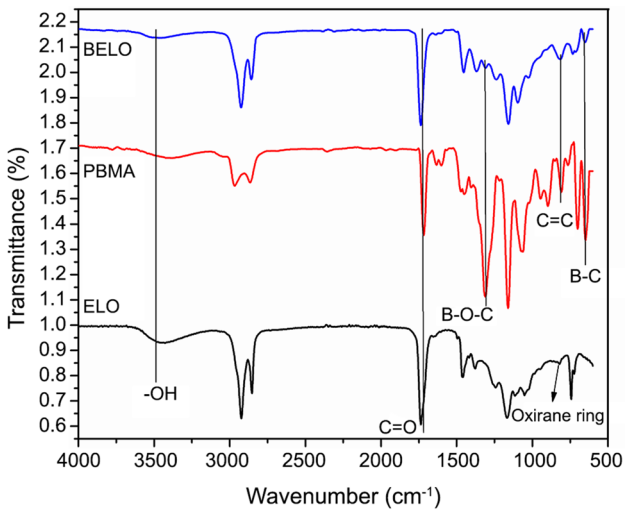

Fig. 2 FTIR analysis of ELO, PBMA, and BELO

Fig. 3 [1]HNMR analysis of ELO

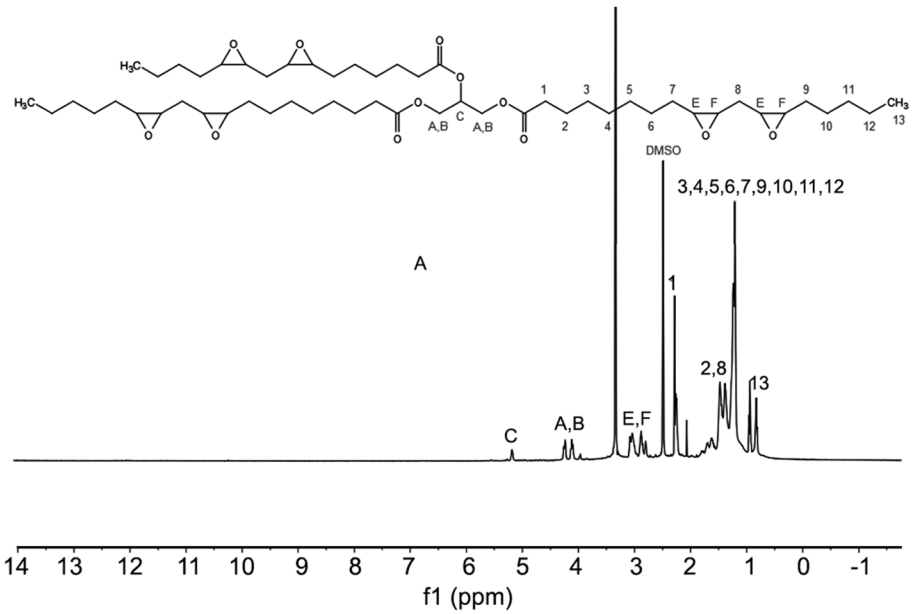

–C–B–O– backbone of BELO oligomer. From the NMR analysis, it is revealed that boron is successfully incorporated into the backbone of BELO oligomer.

BELO curing study by FTIR

In UV-curing process, a liquid coating is exposed to UV light to be converted into a solid coating. The crosslinking reactions are originated from acrylate double bonds when exposed to UV light. The extent of double bond conversion was calculated using FTIR spectra shown in Fig. 7. Before exposure to UV light, the FTIR spectrum BELO oligomer showed a peak at 808 cm^{-1} which could be attributed to the C=C vibration of acrylate. The FTIR spectra of the UV-cured coating showed the complete disappearance of the absorption peak at 808 cm^{-1}, that means no C=C bonds remained in the backbone [40, 41]. Thus, it can be concluded that the crosslinking reaction takes place through the double bonds of BELO oligomer when it is exposed to UV light.

Mechanical properties

The resulting coatings were characterized for their mechanical and optical properties and the results are given in Table 3. As seen in the table, the gloss of UV-cured coatings decreases with increasing BELO content. All coatings show a pencil hardness above 3H, which is due to the high crosslinking density of the cured coating network. PUA40 coating shows higher hardness value compared to PUA, PUA10, PUA20 and PUA30 coatings. The excellent adhesion of coatings to wood substrate was evaluated by cross-cut adhesion test. The secondary hydroxyl groups present in the polymer backbone which facilitates the hydrogen bonding interactions between the coating and wood substrate improves the adhesion properties [42].

Table 3 Mechanical properties of PUA, PUA10, PUA20, PUA30 and PUA40 coatings

Properties	PUA	PUA10	PUA20	PUA30	PUA40
Gloss (60°)	112.2	104.9	101.2	102.3	101.4
Cross-cut adhesion	Pass	Pass	Pass	Pass	Pass
Pencil hardness	3H	3H	4H	5H	5H

Solvent resistance

All coatings were tested for 200 cycles of solvent scrub (MEK) and a good solvent scrub resistance was observed for them. This could be attributed to the highly cross-linked structure of coatings. In addition, the coatings have N–H and –OH groups present in their backbone, which create hydrogen bonding interactions that are either intermolecular or intramolecular, and therefore, enhance the scrub resistance properties of the coatings [43]. The scrub resistance results revealed that the UV-curable PUA- and BELO-incorporated PUA coatings had an excellent cross-linked structure, which could resist against solvent scrub resistance test.

Stain resistance

Stain resistance of coatings was evaluated using a permanent ink, ballpoint ink, turmeric, tea and shoe polish, and the obtained results are tabulated in Table 4. As seen in the table, by increasing the BELO percentage in the PUA formulations, the stain resistance has improved up to a certain

Table 4 Stain resistance of PUA, PUA10, PUA20, PUA30 and PUA40 coatings

Coatings	Turmeric	Shoe polish	Permanent ink	Ballpoint ink	Tea
PUA	5	4	3	5	5
PUA10	5	5	4	5	5
PUA20	5	5	4	5	5
PUA30	5	5	5	5	5
PUA40	5	5	5	5	5

3 poor, *4* satisfactory, *5* good

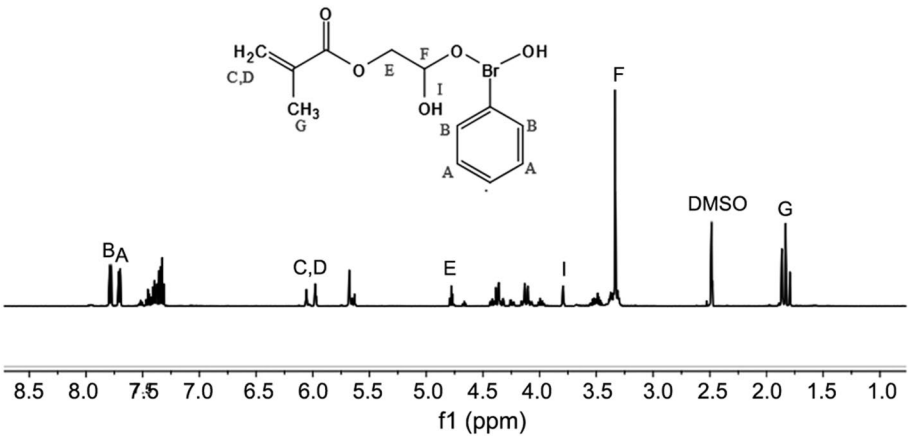

Fig. 4 ^{1}HNMR analysis of PBMA

extent, which may be attributed to the formation of more compact three-dimensional interpenetrating networks.

Thermal properties

As seen in Fig. 8, the T_g values of PUA, PUA10, PUA20, PUA30 and PUA40 coatings are 44, 44, 46, 47 and 57 °C, respectively. The increase in T_g values is due to increase in the percentage of BELO in PUA coating formulations. It should be noted that the crosslink density of the PUA coatings is directly proportional to the percentage of BELO, and hence, PUA40 coating showed higher T_g compared to the PUA, PUA10, PUA20 and PUA30 coatings. The TGA curves of cured coatings, shown in Fig. 9, provide information about the thermal stability in terms of weight loss as a function of temperature. Thermal stability is enormously affected by the number of hard and soft segments present in the coating structure. It has to be emphasized that, the urethane linkage and structure of isocyanate used are responsible for existing hard segments, and long aliphatic chains are responsible for soft segments. The value of 5 wt% loss degradation temperature (T_d 5%) of the cured coatings increased from 227.30 °C for PUA coating to 330.17 for PUA40 coating. Statistic heat resistance, 5% (T_d 5%) and 30% (T_d 30%) weight loss temperature and char yield at 600 °C are tabulated in Table 5. The calculated T_s value has increased from 159.45 to 185.46 °C with increase in BELO content in PUA coating, while the thermal resistance properties of coating are enhanced with increase in crosslink density. From the TGA curves it can be concluded that, PUA40 coating has higher thermal resistance properties compared to the PUA, PUA10, PUA20 and PUA30 coatings, with the possible reason being that the percentage of BELO is having an impact on the crosslink density of the cured coating. In addition, the aromatic ring of PBA enhances the thermal resistance properties of the coating [44–46]. It can be observed that, higher char yield is obtained with increase in the BELO content.

Table 5 TGA analysis of PUA, PUA10, PUA20, PUA30 and PUA40 coatings

Coatings	5% (°C)	30% (°C)	T_s (°C)	Residues (%) at 600 °C
PUA	227.30	390.83	159.45	3.981
PUA10	248.58	405.31	167.88	4.285
PUA20	284.16	405.98	175.05	4.555
PUA30	294.64	404.31	176.61	4.118
PUA40	330.17	410.71	185.46	5.197

LOI and UL-94 analysis

The flame retardancy of the coatings was evaluated by LOI test, and the results are shown in Fig. 10. The LOI values are

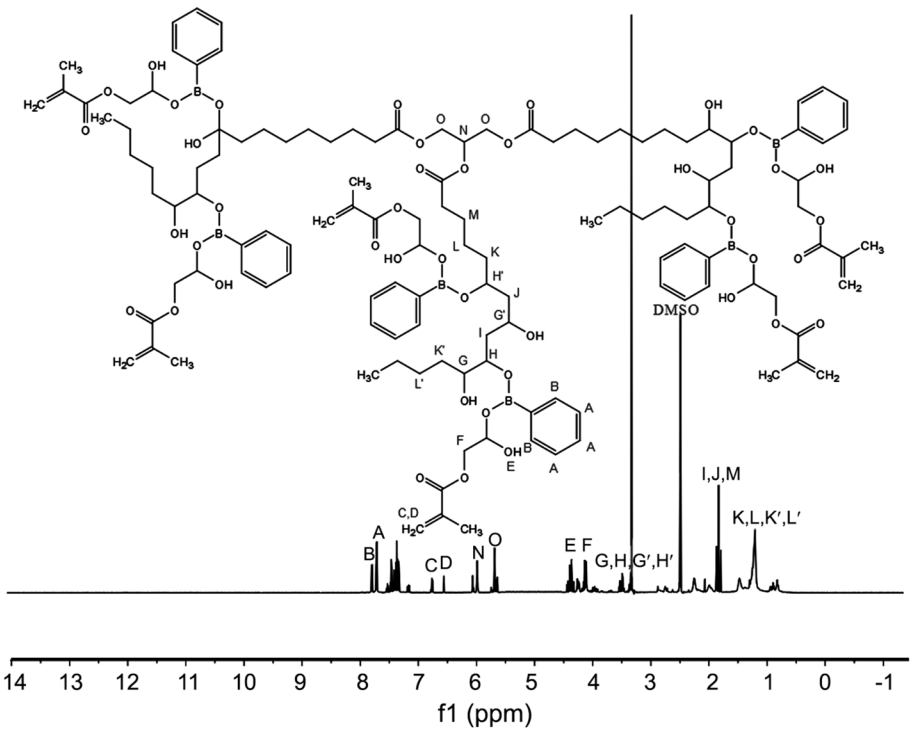

Fig. 5 ^{1}HNMR analysis of BELO

increased from 19 to 25 with increases in BELO oligomer content in the UV-curable PUA coating formulation. The high LOI value of 25, which belongs to the PUA4 coating, is due to the highest content of BELO oligomer in this formulation. The improvement in the flame-retardancy performance of the coating with the addition of BELO may be due to the boron which acts as a flame retardant in both condensed and vapor phases. During firing, the endothermic dehydration reaction of boron will take place, and so the heat of combustion is absorbed. Thus, the released water vapor will dilute the oxygen and the other flammable gases during firing. This flame inhibition mechanism justifies vapor phase barrier action, during the formation of boron oxide on combustion, which works as a protective barrier against the fire into the condensed phase and the mechanism highlights that prohibiting the heat transfer and slow spreading of the flames develops a barrier against the flame [47]. The residual char yield of coatings increased as the content of BELO in the PUA oligomer was increased, therefore the heat transfer from the source to the substrate was prevented and the flame retardancy of the coatings was improved. This conclusion is in accordance with the char yield data obtained from the TGA analysis, which indicated that the flame-retardancy performance of coating improved with increase in BELO oligomer content [33, 48]. All coatings were characterized by the UL-94 test and all UV-cured coatings showed self-extinguishing behavior except PUA and PUA10 coatings. The coatings that exhibited self-extinguishing behavior were able to quench the fire within a period of 8–12 s after the flame was removed during the test. There was no dripping char residue after completion of burning test, indicating the good structural stability of residual char which is the consequence of increased boron content and molecular structure of PUA oligomer.

Characterization of residual char structure by FTIR and microscopic analysis

As shown in Fig. 11, the structure of residual char after UL94 test was analyzed by FTIR to understand the role of boron-containing flame-retardant system in the thermo-oxidative degradation process. The peaks at 2925 and 2847 cm^{-1} are due to the asymmetric and symmetric vibrations of CH_2 groups having remained after the thermo-oxidative degradation. The FTIR spectra show a peak at 1629 cm^{-1} which can be assigned to the C=C stretching of aromatic ring. In addition, the intensity of this peak increases with increase in the boron compound content. The absorption bands of N–H, B–O and B_2O_3 are overlapped in the 3200–3600 cm^{-1} range. The peaks at 3224 and 3378 cm^{-1} belong to B–O and B_2O_3 [49, 50]. As the FTIR results reveal, the chemical structure of char alters with the addition of BELO oligomer. The SEM images of the char residues of PUA and PUA40 coatings obtained from UL-94 test are shown in Fig. 12. It is observed that the surface structure of PUA residual char changes with increases in boron-containing flame-retardant oligomer content. The SEM images of PUA char show a number of holes on the surface, through which gas can escape during

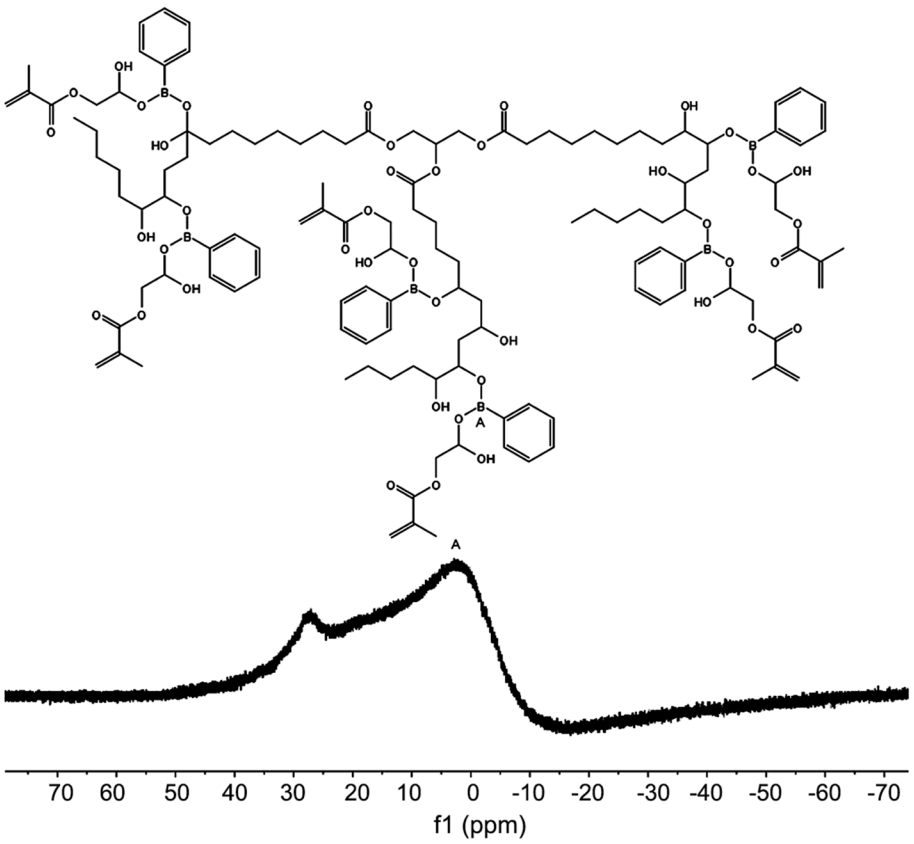

Fig. 6 ^{11}B NMR analysis of BELO

the combustion process. On the other hand, PUA40 coating exhibited a very close and dense carbonaceous char compared to the PUA coating. A dense carbonaceous char can enhance the flame-retardancy property by reducing the rate of flame propagation and heat transfer [51]. According to the microscopic study of morphology shown in Fig. 6, the flame-retardancy performance was improved with the addition of BELO oligomer in PUA coatings.

Conclusion

The boron-containing UV-curable oligomer was successfully synthesized using linseed oil, phenylboronic acid, and glycidyl methacrylate. After synthesis, the boron-containing UV-curable oligomer was characterized by physicochemical methods and further confirmed by FTIR, ^{1}H, and ^{11}B NMR spectroscopy. The synthesized boron-containing UV-curable oligomer was incorporated into the conventional PUA at different concentrations, and then its effect on the coating properties was studied. In the UV-cured system, the conversion of double bond was studied by FTIR measurement. The TGA analysis demonstrated that by increase in boron-containing UV-curable oligomer content in the conventional PUA coatings, the thermal properties were improved and char content was increased. The boron-containing UV-curable oligomer-incorporated PUA coatings showed better mechanical, stain resistance and solvent resistance properties as compared to the conventional PVA coating. The LOI value of coatings increased from 19 to 25 as the BELO oligomer content was increased. The LOI and UL-94 tests results showed that by increasing the BELO oligomer content, the flame-retardant performance of UV curable

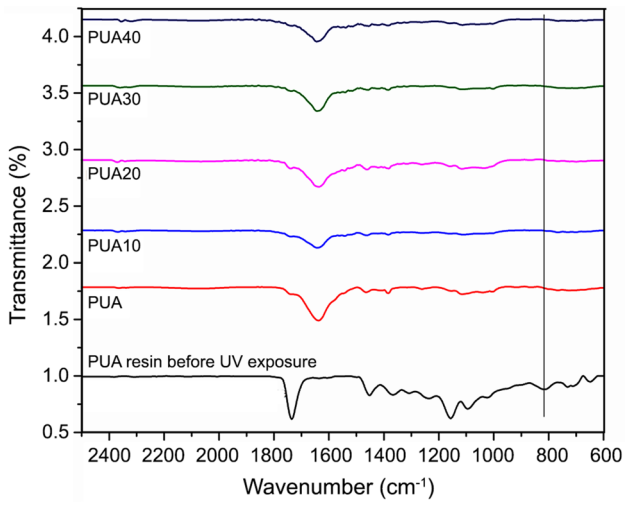

Fig. 7 Unsaturation conversion study by FTIR spectra

coatings was improved. The proposed work opens the doors to many new directions of research in bio-based materials (Figs. 7, 8, 9, 10, 11, 12).

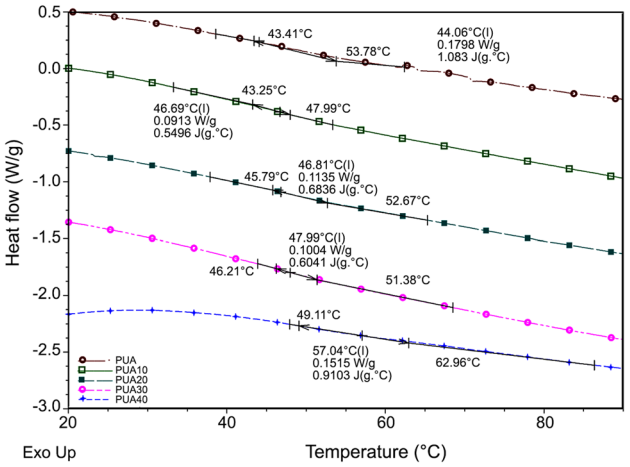

Fig. 8 DSC analysis of coatings

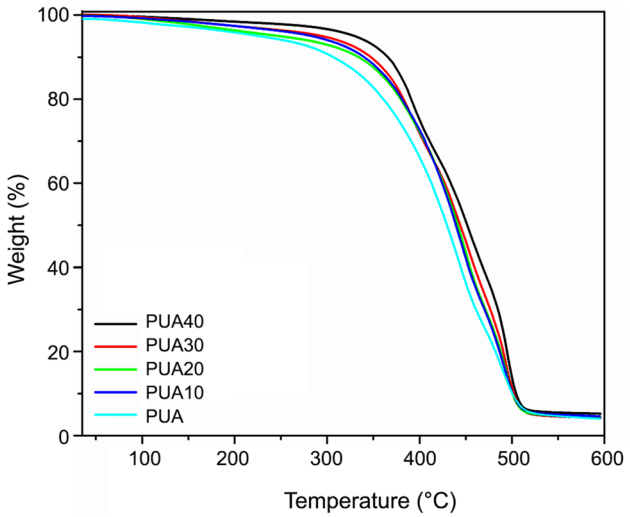

Fig. 9 TGA analysis of coatings

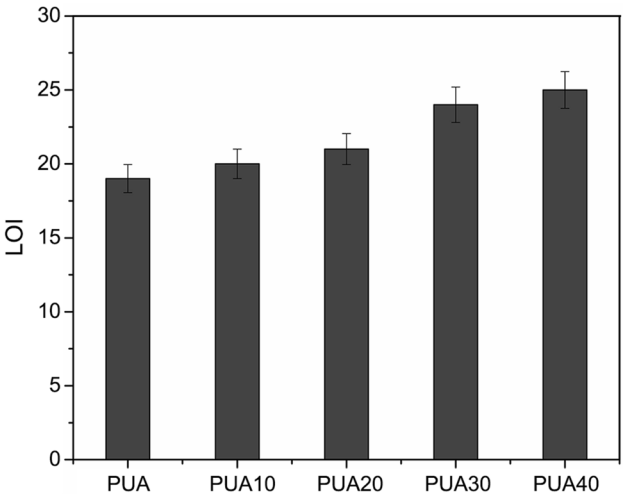

Fig. 10 LOI analysis of coatings

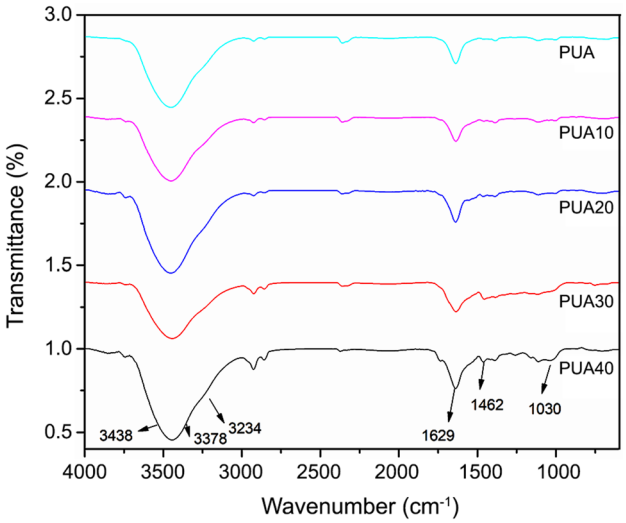

Fig. 11 FTIR analysis of residual char

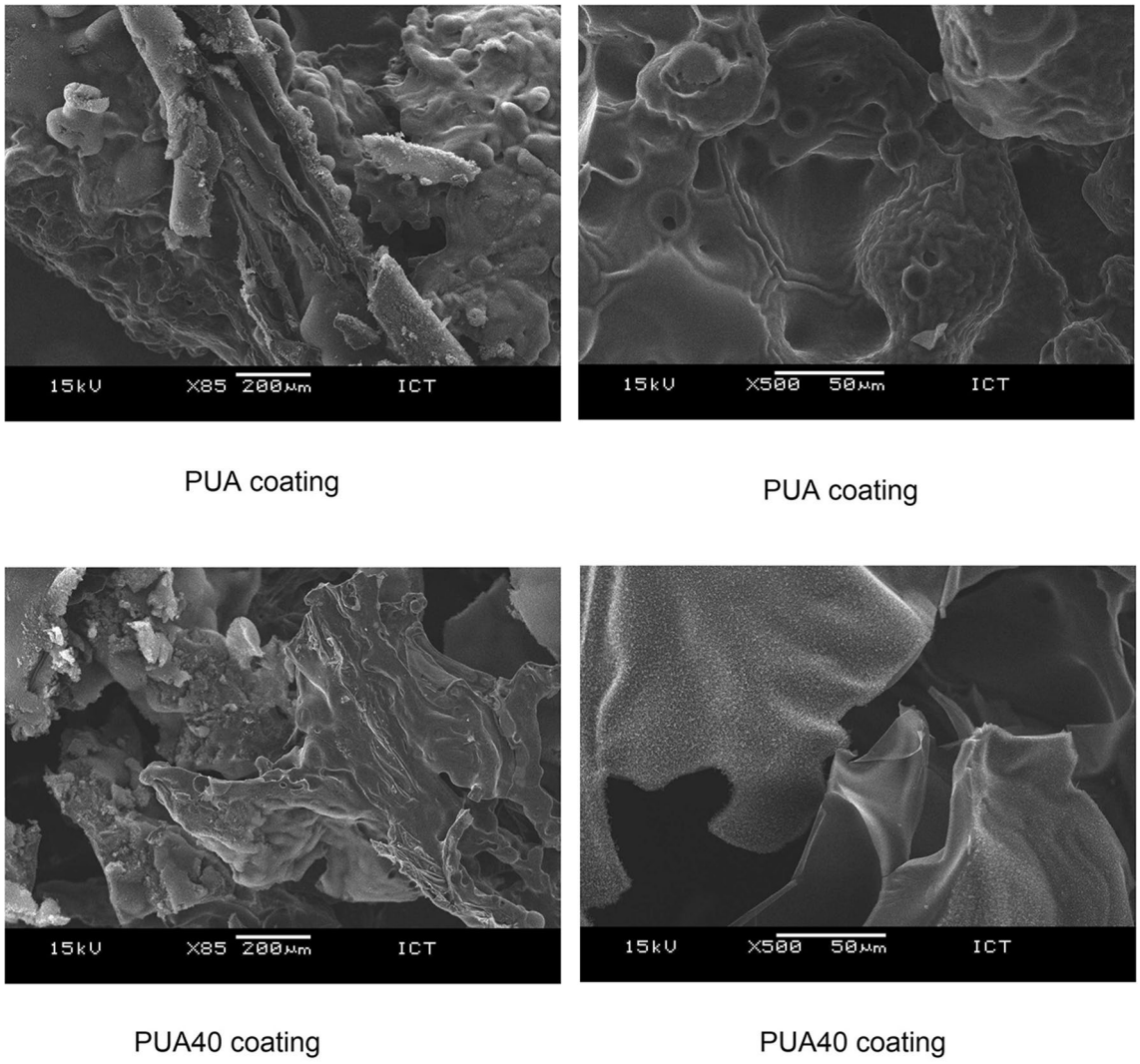

Fig. 12 SEM analysis of residual char of PUA and PUA40 after UL-94 tests

References

1. Chambhare S, Lokhande G, Jagtap RN (2016) Design and UV-curable behavior of boron-based reactive diluent for epoxy acrylate oligomer used for flame retardant wood coating. Des Monomers Polym 20(1):125–135
2. Laoutid F, Bonnaud L, Alexandre M, Lopez-Cuesta J, Dubois PH (2009) New prospects in flame-retardant polymer materials: from fundamentals to nanocomposites. Mater Sci Eng R 63:100–125
3. Hull TR, Witkowski A, Hollingbery L (2011) Fire retardant action of mineral fillers. Polym Degrad Stab 96:1462–1469
4. Randoux TH, Vanovervelt JCL, Bergen HVD, Camino G (2002) Halogen-free flame retardant radiation curable coatings. Prog Org Coat 45:281–289
5. Rakotomalala M, Wagner S, Doring M (2010) Recent developments in halogen free flame retardants for epoxy resins for electrical and electronic applications. Material 3:4300–4327
6. Ferre-Huguet N, Nadal M, Schuhmacher M, Domingo JL (2006) Environmental impact and human health risks of polychlorinated dibenzo-*p*-dioxins and dibenzofurans in the vicinity of a new hazardous waste incinerator: a case study. Environ Sci Technol 40:61–66
7. Liu J, Tang J, Wang X, Wu D (2012) Synthesis, characterization and curing properties of a novel cyclolinear phosphazene-based epoxy resin for halogen-free flame retardancy and high performance. RSC Adv 2:5789–5799
8. Menard R, Negrell C, Fache N, Ferry L, Sonnier R, David G (2015) From a bio-based phosphorus-containing epoxy monomer to fully bio-based flame-retardant thermosets. RSC Adv 5:70856–70867
9. Cakmakci E, Kahraman MV (2015) In: Tiwari A, Polycarpov A (eds) Boron/phosphorus-containing flame-retardant photocurable coatings. Royal Society of Chemistry, London
10. Van Krevelen DW (1975) Some basic aspects of flame resistance of polymeric materials. Polymer 16:615–620
11. Sacristan M, Hull T, Stec A, Ronda J, Galia M, Cadiz V (2010) Cone calorimetry studies of fire retardant soybean-oil-based

copolymers containing silicon or boron: comparison of additive and reactive approaches. Polym Degrad Stab 95:1269–1274
12. Singh AP, Gunasekaran G, Suryanarayana C, Naik RB (2015) Fatty acid based waterborne air drying epoxy ester resin for coating applications. Prog Org Coat 87:95–105
13. Saeed A, Shabir G (2013) Synthesis of thermally stable high gloss water dispersible polyurethane/polyacrylate resins. Prog Org Coat 76:1135–1143
14. Barbara P, Michal K, Ewa O, Szczepan Z (2016) Structure and properties of polyurethane-based powder clear coatings systems modified with hydrotalcites. Prog Org Coat 95:120–126
15. Hwang HD, Kim HJ (2011) Enhanced thermal and surface properties of waterborne UV-curable polycarbonate-based polyurethane (meth)acrylate dispersion by incorporation of polydimethylsiloxane. React Funct Polym 71:655–665
16. Liu R, Zhang X, Zhu J, Liu X, Wang Z, Yan J (2015) UV-curable coatings from multiarmedcardanol-based acrylate oligomers. ACS Sustain Chem Eng 3:1313–1320
17. Zhao L, Wei M, Nie J, He Y (2016) Cationic UV-curable fluorine containing polyacrylic epoxy prepolymer with good compatibility. Prog Org Coat 100:70–75
18. Wang X, Xing W, Song L, Yu B, Hu Y, HengYeoh G (2013) Preparation of UV-curable functionalized graphene/polyurethane acrylate nanocomposite with enhanced thermal and mechanical behaviors. React Funct Polym 73:854–858
19. Swiderski KW, Khudyakov IV (2004) Synthesis and properties of urethane acrylate oligomers: direct versus reverse addition. Ind Eng Chem Res 43:6281–6284
20. Okkerse C, van Bekkum H (1999) From fossil to green. Green Chem 1:107–114
21. Dai J, Jiang Y, Liu X, Wang J, Zhu J (2016) Synthesis of eugenol-based multifunctional monomers via a thiol-ene reaction and preparation of UV curable resins together with soybean oil derivatives. RSC Adv 6:17857–17866
22. Fertier L, Koleilat H, Stemmelen M, Giani O, Joly-Duhamel C, Lapinte V, Jean-Jacques R (2013) The use of renewable feedstock in UV-curable materials—a new age for polymers and green chemistry. Prog Polym Sci 38:932–962
23. Ferdosian F, yuan Z, Anderson M, Chunbao X (2015) Sustainable lignin-based epoxy resins cured with aromatic and aliphatic amine curing agents: curing kinetics and thermal properties. Thermochim Acta 618:48–55
24. Aouf C, Nouailhas H, Fache M, Sylvain C, Bernard B, Helene F (2013) Multi-functionalization of gallic acid. Synthesis of a novel bio-based epoxy resin. Eur Polym J 49:1185–1195
25. Gubbels E, Drijfhout JP, Posthuma-van Tent C, Jasinska-Walc L, Noordover BA, Koning CE (2014) Biobased semi-aromatic polyesters for coating applications. Prog Org Coat 77:277–284
26. Farmer TJ, Castle RL, Clark JH, Duncan J (2015) Synthesis of unsaturated polyester resins from various bio-derived platform molecules. Int J Mol Sci 6:14912–14932
27. Han L, Dai J, Zhang L, Songqi MA, Jun D, Zhang R, Zhu J (2014) Diisocyanate free and melt polycondensation preparation of bio-based unsaturated poly(ester-urethane)s and their properties as UV curable coating materials. RSC Adv 4:49471–49477
28. Mahapatra SS, Karak N (2004) Synthesis and characterization of polyesteramide resins from Nahar seed oil for surface coating applications. Prog Org Coat 51:103–108
29. Chiellini E, Chiellini F, Cinelli P (2002) Polymers from renewable resources. In: Scott G (eds) Degradable polymers. Springer, Dordrecht
30. Belgacem M, Gandini A (2008) Monomers, polymers and composites from renewable resources. Elsevier, Amsterdam
31. Sharmin E, Zafar F, Akram D, Manawwer A, Sharif A (2015) Recent advances in vegetable oils based environment friendly coatings: a review. Ind Crop Prod 76:215–229
32. Martini D, Braga B, Samios D (2009) On the curing of linseed oil epoxidized methyl esters with different cyclic dicarboxylic anhydrides. Polymer 50:2919–2925
33. Marta S, Joan C, Marina G, Virginia C (2010) Synthesis and properties of boron-containing soybean oil based thermosetting copolymers. Polymer 51:6099–6106
34. Cakmakc E, Mulazim Y, Kahraman MV, Apohan NK (2012) Preparation and characterization of boron containing thiol-ene photocured hybrid coatings. Prog Org Coat 75:28–32
35. Emre B, Tulay I, Attila G (2013) Flame retardant UV-curable acrylated epoxidized soybean oil based organic–inorganic hybrid coating. Prog Org Coat 76:985–992
36. Patil DM, Phalak GA, Mhaske ST (2017) Design and synthesis of bio-based UV curable PU acrylate resin from itaconic acid for coating applications. Des Monomers Polym 20:269–282
37. Diez-Pascual AM, Diez-Vicente AL (2015) Development of linseed oil–TiO_2 green nanocomposites as antimicrobial coatings. J Mater Chem B 3:4458–4471
38. Gogoi P, Boruah M, Sharma S, Dolui SK (2015) Blends of epoxidized alkyd resins based on Jatrophaoil and the epoxidized oil cured with aqueous citric acid solution: a green technology approach. ACS Sustain Chem Eng 3:261–268
39. Feng L, Xing-Rong Z, Hong-QiangL (2012) Synthesis and properties of UV curable polyurethane acrylates based on two different hydroxyethyl acrylates. J Cent South Univ 19:911–917
40. Choi YS, Kim KH, Kim DG, Kim HJ, Cha SH, Lee JC (2014) Synthesis and characterization of self-cross-linkable and bactericidal methacrylate polymers having renewable cardanol moieties for surface coating applications. RSC Adv 4:41195–41203
41. Phalak G, Patil D, Vignesh V, Mhaske S (2018) Development of tri-functional biobased reactive diluent from ricinoleic acid for UV curable coating application. Ind Crop Prod 119:9–21
42. Manfredi LB, Fraga AN, Vazquez A (2006) Influence of the network structure and void content on hygrothermal stability of resol resin modified with epoxy-amine. J Appl Polym Sci 102:588–597
43. Kathalewar M, Sabnis A, D'Melo D (2014) Polyurethane coatings prepared from CNSL based polyols: synthesis, characterization and properties. Prog Org Coat 77:616–626
44. Shukla SK, Srivastava K, Srivastava D (2015) Studies on the thermal, mechanical and chemical resistance properties of natural resource derived polymers. Mater Res 18:1217–1223
45. Balgude D, Sabnis A, Ghosh SK (2016) Synthesis and characterization of cardanol-based aqueous 2K polyurethane coatings. Eur Polym J 85:624–634
46. Choi J, Seo J, Khan S (2011) Effect of acrylic acid on the physical properties of UV-cured poly(urethane acrylateco-acrylic acid) films for metal coating. Prog Org Coat 71:110–116
47. Osman P, Cevdet K (2014) Use of boron oxide and boric acid to improve flame retardancy of an organophosphorus compound in neat and fiber reinforced polyamide6. J Vinyl Add Technol 22:300–310
48. Liua R, Luo J, Ariyasivam S, Liu X, Chen Z (2017) High biocontent natural plant oil based UV-curable branched oligomers. Prog Org Coat 105:143–148
49. Shuo T, Lijun Q, Yong Q, Yuping D (2018) Synergistic flame-retardant effect and mechanisms of boron/phosphorus compounds on epoxy resins. Polym Adv Technol 29:641–648
50. Murat S, Umit U, Bekir T, Mehmet Y D (2016) Effect of boron compounds on fire protection properties of epoxy based intumescent coating. Fire Mater 41:17–28
51. Benjamin T, Bin Y, Wai Yi C, Shuk Ying C, Wei Y, Bin F (2018) Synthesis and application of synergistic azo-boron-BPA/polydopamine as efficient flame retardant for poly(lactic acid). Polym Degrad Stab 152:64–74